

## Optical Absorption and Luminescence of Irradiated $\text{MgF}_2$ †

O. E. FACEY AND W. A. SIBLEY

*Solid State Division, Oak Ridge National Laboratory, Oak Ridge, Tennessee 37830*

(Received 2 May 1969)

A study of the temperature and polarization dependence of the absorption and luminescence from electron and neutron-irradiated  $\text{MgF}_2$  crystals has been made. The absorption band at 260 nm is accepted as due to an  $F$  center, and excitation, when other centers are absent, produces an emission at about 430 nm. Two other absorption bands at 370 and 400 nm arise from different types of  $M$  centers, and our data suggest that these centers give rise to emission bands at 420 and 600 nm, respectively. Several narrow absorption lines are observed in both electron- and neutron-irradiated samples. From polarization studies and optical bleaching treatment, the lines at 387.2, 385.7, 384.5, 382.3, and 380.8 nm are identified as zero-phonon and phonon-assisted transitions of the defect responsible for the 370-nm band. A comparison is made between the vibrational energies associated with the phonon-assisted lines and the dispersion relationships calculated for  $\text{MgF}_2$ .

### I. INTRODUCTION

IN the past few years several rather detailed studies on the coloration of  $\text{MgF}_2$  single crystals have been made.<sup>1-3</sup> In these crystals the  $F$  center is expected to have a  $C_{2v}$  symmetry due to the cassiterite structure of the lattice and there are four possible types of  $M$  centers each with a different symmetry. Blunt and Cohen<sup>1</sup> made a systematic investigation of the optical absorption and emission of irradiated samples at room temperature, and on the basis of their data identified an absorption band at about 260 nm as being due to  $F$ -center absorption. When the electric vector  $\mathbf{E}$  of the incident light was perpendicular to the  $c$  axis of the crystal ( $\mathbf{E} \perp c$ ), the band appeared at 255 nm; but when light with  $\mathbf{E} \parallel c$  was used, the peak was observed at 265 nm. They attributed two other bands, 320 and 370 nm, to  $M$ -center absorption. Both of these bands are polarized such that they are only detected with light oriented with  $\mathbf{E} \perp c$ . Blunt and Cohen observed another band at 300 nm, but did not assign it to any particular defect. Recently,<sup>2,4</sup> another absorption band at 400 nm has been found in both neutron and electron irradiated  $\text{MgF}_2$ . This band has been assigned to an  $M$ -center absorption.

A survey of the room temperature luminescence from irradiated  $\text{MgF}_2$  was also made by Blunt and Cohen.<sup>1</sup> They reported that emission bands at about 420 and 600 nm were excited by all of the broad lines available from a high-pressure mercury arc below the 405-nm line. Light of the 405- and 436-nm mercury lines excited only the yellow 600-nm band. Moreover, it was found that the 600-nm emission was essentially independent of the polarization of the incident light, whereas the 420-nm band was excited principally by light with  $\mathbf{E} \perp c$ .

In the last year, very narrow absorption lines have been reported to occur in both electron<sup>3</sup> and neutron irradiated<sup>3,4</sup> crystals. The existence of these sharp lines makes it possible to obtain more detailed information about radiation defects and their interaction with the crystal lattice than can be determined from broad band spectra only. The purpose of this paper is to investigate both the absorption and luminescence from electron and neutron irradiated  $\text{MgF}_2$  crystals and to assign the observed absorption and luminescence bands to specific defects. A study of the sharp line absorption is also made and in one case it is possible to connect some of these lines with a broad absorption band.

### II. PROCEDURE

Single-crystal ingots of  $\text{MgF}_2$  were obtained from the Harshaw Chemical Co., Optovac Corporation, and Alpha Inorganic. Table I shows the impurities in these crystals as detected by emission spectroscopy and mass spectroscopy. The ingots were cut into oriented optical specimens with thicknesses ranging from 0.5 to 2.0 mm. Some of the samples were cut so that the crystal faces were perpendicular to the  $c$  axis ( $c_{\perp}$ ) and others so that the faces were parallel to the  $c$  axis ( $c_{\parallel}$ ). Optical-absorption measurements were made with a Cary 14R spectrophotometer. For polarization work a pair of Polaroid ultraviolet-type HNP'B unsupported polarizers were used in both the sample and reference beams. When high resolution was desired the spectrophotometer was run with slits at less than 0.005 mm (a resolution of about 0.1 nm at 400 nm). Luminescence data were taken using either an EMI 9558Q or an RCA 7102 multiplier phototube mounted to a  $\frac{1}{2}$ -m Bausch & Lomb monochromator. Both tubes were cooled to dry ice temperature to reduce dark current. The detection system was calibrated using a standard quartz-iodine lamp with calibration traceable to the Bureau of Standards.<sup>5</sup> The resolution of the system was about 1.5 nm at 400 nm when band shapes were taken. A mercury lamp mounted to another  $\frac{1}{2}$ -m monochromator

† Research sponsored by the U. S. Atomic Energy Commission under contract with Union Carbide Corporation.

<sup>1</sup> R. F. Blunt and M. I. Cohen, *Phys. Rev.* **153**, 1031 (1967).

<sup>2</sup> W. A. Sibley and O. E. Facey, *Phys. Rev.* **174**, 1076 (1968).

<sup>3</sup> O. E. Facey, D. L. Lewis, and W. A. Sibley, *Phys. Status Solidi* **32**, 831 (1969).

<sup>4</sup> M. Nakagawa and K. Ozawa, in *International Symposium on Color Centers in Alkali Halides*, Rome, 1968, Abstract No. 140 (unpublished).

<sup>5</sup> R. Stair, W. E. Schneider, and J. K. Jackson, *Appl. Opt.* **2**, 1151 (1963).

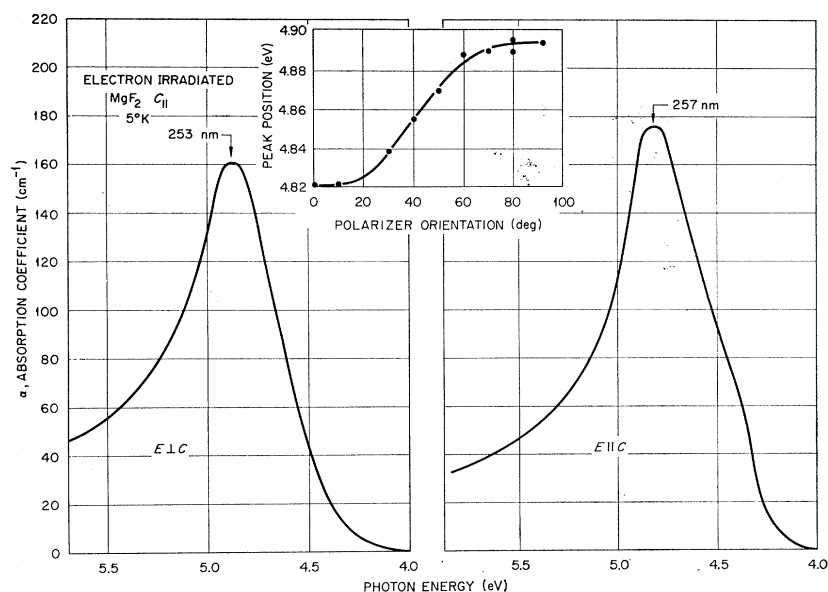


FIG. 1. Optical absorption at 5°K in the range 4.0–5.5 eV for an electron irradiated sample for two polarizations of the incident light.

mator and a GE LC-90 industrial x-ray unit (90 kV and 3–5 mA) were used to stimulate luminescence in the crystals. Both optical-absorption and luminescence measurements were made with the samples mounted in a Sulfran liquid-helium cryostat and the sample temperature was fixed by using constant temperature refrigerants. Specimen temperatures were measured using a Pt-resistance thermometer.

The crystals were irradiated at 300°K with 1.8-MeV electrons from a Van de Graaff accelerator or at 310°K in the hydraulic tube system No. 1-F-8 tube 12 of the Oak Ridge Reactor with a flux of  $2.3 \times 10^{13}$  neutrons/cm<sup>2</sup> sec ( $E > 1$  MeV). It was necessary to anneal the neutron irradiated specimens in order to detect some of the zero-phonon lines. This was done in air with the temperature measured by a Chromel-Alumel thermocouple and the furnace regulated to within  $\pm 3^\circ$ K of the desired temperature.

### III. EXPERIMENTAL RESULTS

#### A. *F* Band

In Fig. 1 the 5°K absorption spectra for two polarizations of an electron irradiated  $c_{11}$ -cut  $MgF_2$  sample are shown. In the figure  $E \perp c$  indicates that the electric vector of the incident light is perpendicular to the  $c$  axis and  $E \parallel c$  that the light is polarized parallel to the  $c$  axis. The inset illustrates how the peak position of the band changes with polarizer orientation. The peak position and width of this band at half-maximum were investigated as a function of temperature. The results are depicted in Fig. 2 where the left ordinate indicates the width at half-maximum and the right ordinate the peak position. The half-width,  $W_{1/2}(T)$ , was determined by fitting the absorption band to a Gaussian curve for each measurement temperature  $T$ . The temperature

dependence of the half-width of the band can be approximated by the expression  $W_{1/2}(T) = W_{1/2}(0) \coth h\nu_0/2kT$  where  $W_{1/2}(0)$  is the width at 0°K. When our data are evaluated in terms of this expression we find  $\nu_0 = 9.0 \times 10^{12}$  sec<sup>-1</sup>.

The luminescence as excited by 254-nm light on an unirradiated sample and a specimen irradiated at 232°K to an *F*-center concentration of about  $10^{16}$  cm<sup>-3</sup> is shown in Fig. 3. A small luminescence band is observed at about 410 nm in the unirradiated crystals. After irradiation 254-nm light excitation yields a luminescence band at about 430 nm.

It is important to note that when 254 nm exciting light was used and absorption bands at 370 and 400 nm were present, both the 420- and 600-nm emission occurred regardless of the polarization of the incident light. Blunt and Cohen<sup>1</sup> reported that as they optically bleached the 260-nm *F* band in these crystals the luminescence induced by a 254-nm excitation decreased as the number of *F* centers decreased. This suggests that *F*-center luminescence could play a role in this case

TABLE I. Impurity analyses of samples ( $\mu$ g/g).

Element	Harshaw	$\alpha$ Inorganic	Optovac
Al	2–10	5–10	...
Ba	<1	<1–10	...
Ca	$\leq 20$	8	...
Co	$\leq 10$	4	...
Cr	<1–9	<1–50	45
Cu	10–40	5, 20	...
Fe	<4	<4–10	150–180
K	3	8	...
Mn	1	3–50	...
Na	<10	<10	69
Mo	<10–60	<10–55	...
Pb	<10	<10	...
Si	100	<10	...
Zn	<100	<100	...

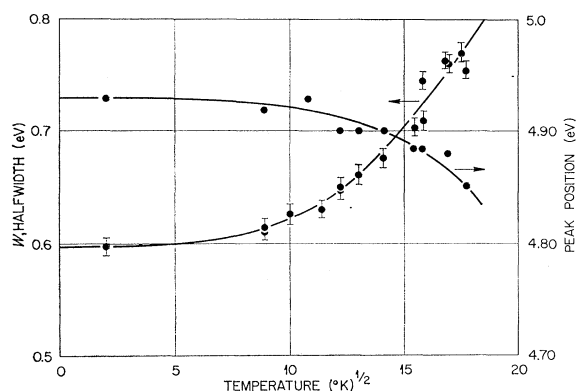


FIG. 2. *F*-Band peak position (right ordinate) and width at half-maximum (left ordinate) as a function of temperature for  $c_1$ .

by stimulating the centers responsible for the 370- and 400-nm bands.

When x-ray excitation was used luminescence bands were observed at 390 nm (3.2 eV) and 590 nm (2.08 eV) in the unirradiated Alpha Inorganic and Optovac samples and only at 390 nm in Harshaw specimens as shown in Fig. 4. The emission from the Harshaw sample was much weaker than that from the others and disappeared when the crystal was irradiated at 232°K. The luminescence at 590 nm has been attributed previously to Mn impurity<sup>6</sup> and as can be seen from Table I this is consistent with the impurity concentrations of the various crystals.

### B. *M* Bands

Two absorption bands which have previously been assigned to *M*-center transitions occur at 370 and 400

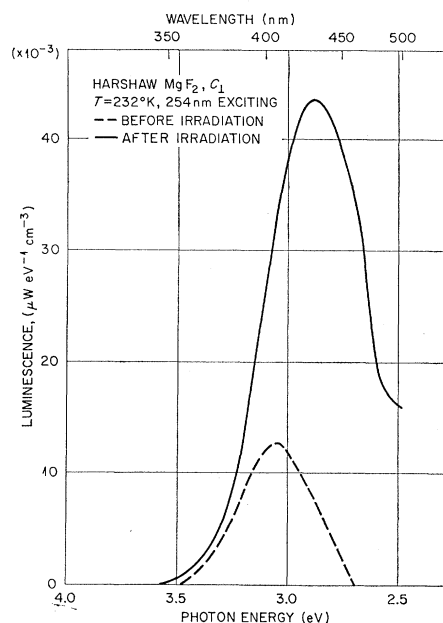


FIG. 3. A plot of luminescence in the range 2.5–4.0 eV as excited by 254-nm light in an unirradiated and an electron irradiated crystal.

nm. Figure 5 shows both of these bands when the sample is at 5°K and the electric vector of the incident light is either parallel or perpendicular to the *c* axis. Some very narrow absorption lines are evident in the vicinity of 390 nm (3.2 eV), the inset portraying these lines in greater detail. It appears that there are lines at 387.2, 384.7, 385.5, 382.3, and 380.8 nm, but, as can be seen, the accuracy with which we can locate some of the lines ( $\pm 0.2$  nm) is not very good, owing

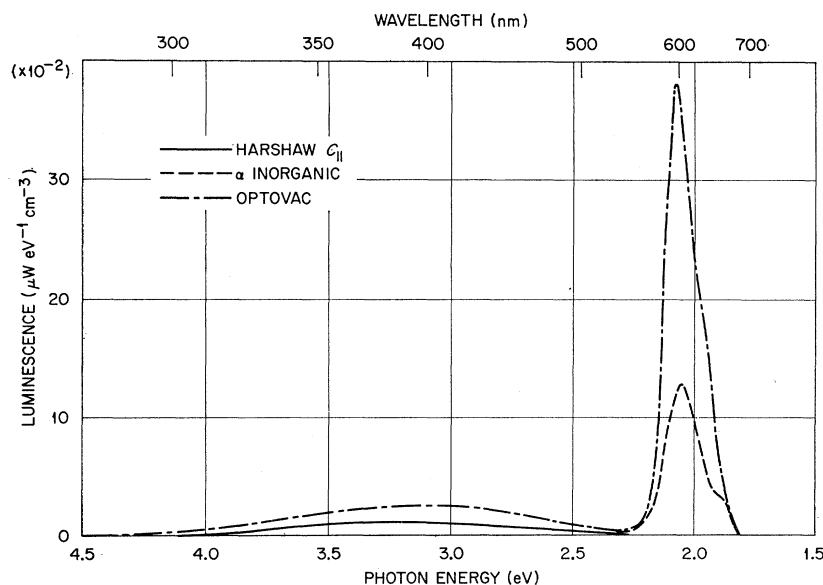


FIG. 4. X-ray-stimulated luminescence for several unirradiated  $MgF_2$  specimens obtained from different sources.

<sup>6</sup> H. W. Leverenz, *Luminescence of Solids* (Wiley-Interscience, Inc., New York, 1950), Table 5.

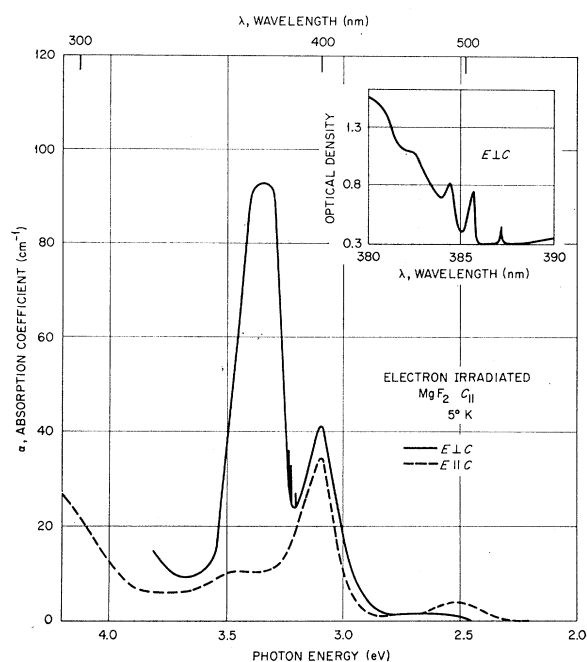


FIG. 5. Optical absorption at 5°K in the range 2.0–4.0 eV for an electron irradiated sample. The inset shows the sharp lines observed in the vicinity of 3.2 eV in greater detail.

to the resolution of the spectrophotometer and the background absorption. It should be noted that these narrow lines only occur for the condition  $E \perp c$  and that the broad band at 370 nm is also polarized with  $E \perp c$ . The 400-nm absorption band is essentially unpolarized. The peak position and width at half-maximum of the 370-nm band was measured as a function of temperature. This is illustrated in Fig. 6. An analysis of these data, similar to that described above for the  $F$  center, yielded  $\nu_q = 8.5 \times 10^{12} \text{ sec}^{-1}$ .

When irradiated specimens are excited with either x-rays or ultraviolet light, emission bands appear at 420 and 600 nm. The emission from a crystal at 5°K excited with 365-nm light is shown in Fig. 7. The solid line is for light emitted with  $E \perp c$  and the dashed line indicates the emission with  $E \parallel c$ . When the electric

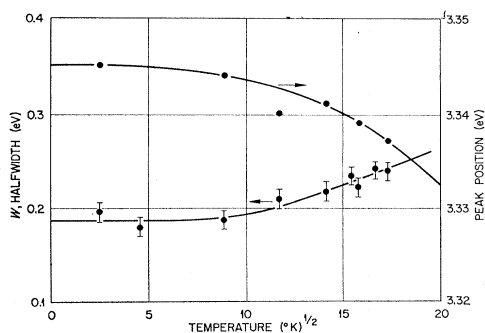


FIG. 6. The peak position and half-width of the 370-nm absorption band as a function of temperature.

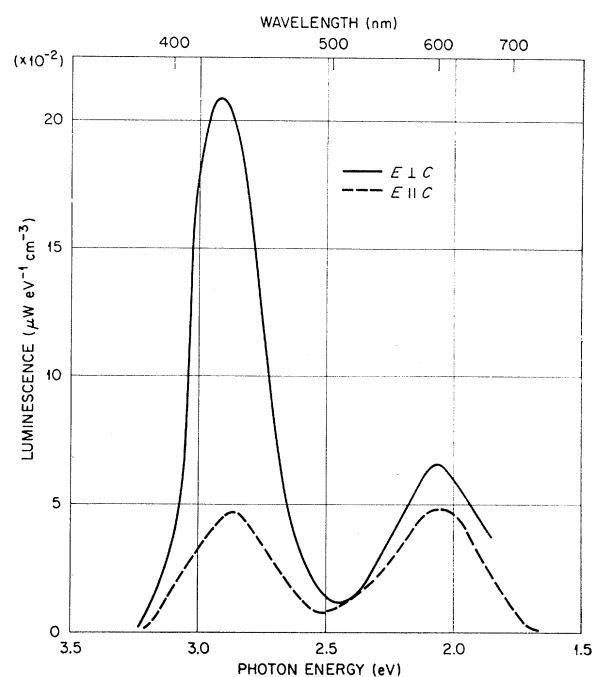


FIG. 7. Optical emission in the range 1.5–3.5 eV stimulated by x ray or 254-nm light excitation. The solid line shows data for the electric vector of the emitted light polarized perpendicular to the  $c$  axis and the dashed line, light parallel to the  $c$  axis.

vector of the exciting light was aligned with the  $c$  axis, it was found that the 420-nm emission band did not occur. The 600-nm band, on the other hand, was essentially independent of polarization. Since the 370-nm absorption band is strongly dichroic it was felt that the 420-nm emission band was most likely associated with the center giving rise to this absorption. Moreover, when the wavelength of the exciting light was changed to 405 nm, so that only a few of the 370-nm centers would be excited, then only the 600-nm emission could be observed. This again indicates that the centers absorbing at 370 and 400 nm give rise to emission at 420 and 600 nm, respectively. Measurements of the peak position and width at half-maximum for the 420-nm luminescence band are shown in Fig. 8.

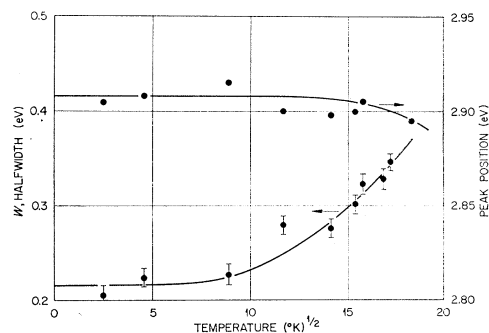


FIG. 8. The peak position and half-width of the 420-nm emission band as a function of temperature.

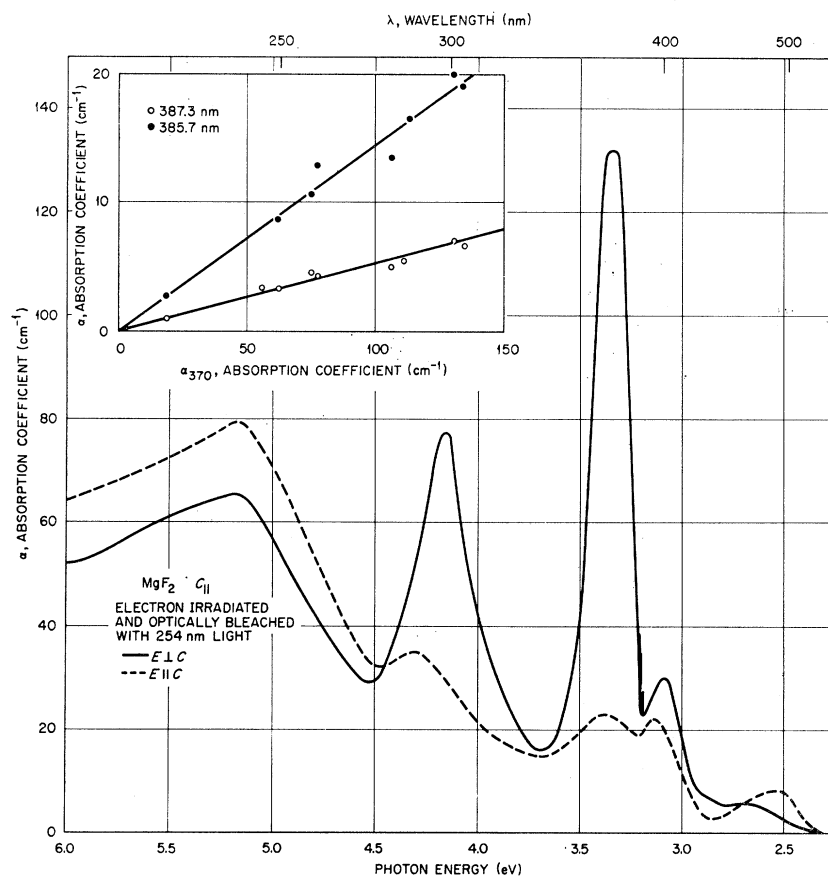


FIG. 9. The optical absorption at 5°K of an electron irradiated crystal optically bleached with 254-nm light at room temperature. The inset shows that as the 370-nm *M*-band absorption increases with bleaching, so do the sharp 387.3- and 385.7-nm lines.

When the half-width data are fit to the expression  $W_{1/2}^2(T) = W_{1/2}^2(0) \coth h\nu_e/2kT$ , then it is found that  $\nu_e = 5.4 \times 10^{12} \text{ sec}^{-1}$ .

### C. Other Bands

Just as in the alkali halides when a sample is illuminated with light of the same wavelength as the *F*-center absorption, there is a decrease in the *F* band and a corresponding increase in the number and type of cluster centers. Figure 9 depicts the absorption spectrum of an optically bleached sample. The *F*-center absorption in the vicinity of 255 nm (4.9 eV) has decreased considerably and bands have appeared around 300 nm (4.2 eV) and 500 nm (2.5 eV). One of the bands occurring around 300 nm is obviously dichroic. The very narrow absorption lines mentioned previously and shown in the inset of Fig. 5 are clearly present in the bleached samples; and, in fact, they increase in size as the 370-nm band increases with bleaching. The inset illustrates that both the 387.3- and 385.7-nm lines increase linearly with the broad 370-nm band which suggests that these lines are associated with the defect responsible for this broad band absorption.

Other bands can also be produced by neutron irradiation of the crystals. Figure 10 shows the  $E \perp c$

and  $E \parallel c$  absorption for an "as irradiated"  $c_{11}$  crystal at 5°K. The most prominent new band is at about 320 nm (3.9 eV) but another band is evident around 280 nm (4.4 eV). The 320-nm band can also be produced by optical bleaching. The narrow lines around 390 nm (3.2 eV) are present in the neutron irradiated crystals just as they are in the electron or gamma irradiated ones. However, the half-widths of these lines are much larger in the neutron irradiated samples suggesting that there is more lattice strain in these samples. When neutron irradiated specimens are annealed to around 630°K, other narrow lines are found to grow in. The lines at 431.7 and 428.8 nm are almost completely polarized, whereas the line occurring at 422.2 nm is not. These lines are shown in the inset of Fig. 10. Further investigation of the 422.2-nm line in a  $c_1$  sample showed no dichroism for the line in this orientation.

### IV. DISCUSSION

As mentioned in the Introduction there are four possible *M*-type centers in  $\text{MgF}_2$ . Figure 11 depicts two adjacent lattice cells in  $\text{MgF}_2$  with the possible *M*-center configurations labeled A, B, C, and D. The centers marked C and B have their dipoles oriented perpendicular to the *c* axis and might be expected to be dichroic. In addition, the *M*(B) center has a  $\langle 110 \rangle$

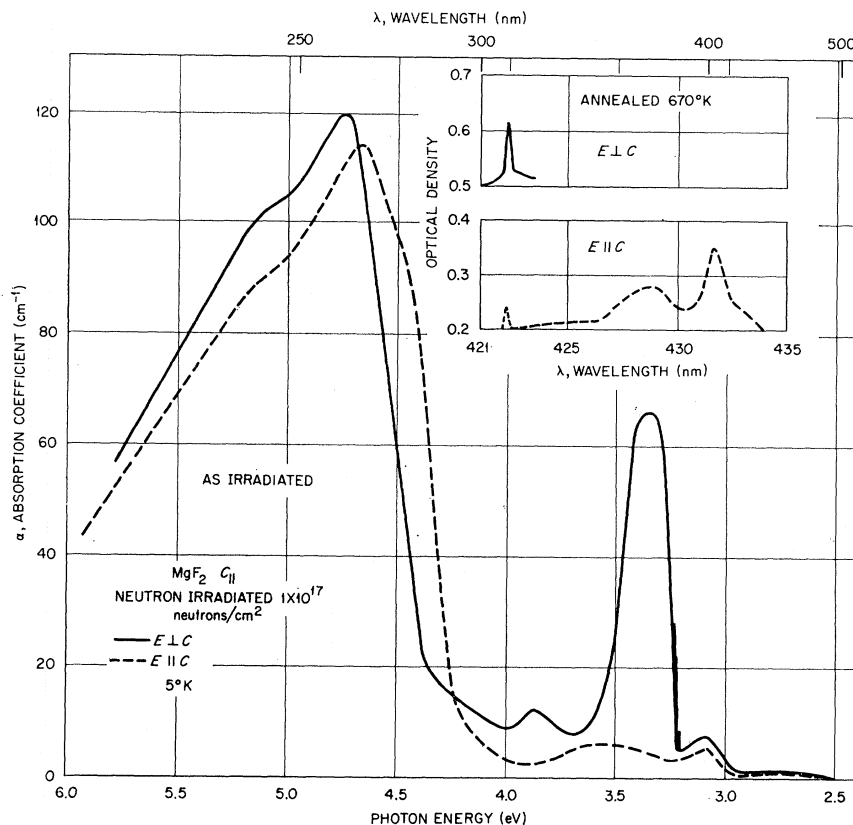


FIG. 10. Optical absorption at 5°K for a neutron irradiated  $MgF_2$  specimen. The inset shows the narrow line absorption observed after neutron irradiated samples have been annealed around 670°K for 10 min.

orientation in the lattice and Blunt and Cohen<sup>1</sup> have shown by preferential bleaching studies on  $c_1$  samples that the 320-nm absorption band is most likely due to this center. This center has a  $D_{2h}$  symmetry and in further discussion we will refer to it as the  $M(D_{2h})$  center. The type-A center has  $C_{2v}$  symmetry, type C has  $C_{2h}$  symmetry, and the symmetry of the type-D center is  $C_1$ . The  $M(C_{2h})$  center should be strongly dichroic in both absorption and emission and we believe on the basis of this work and previous investigations that it is responsible for the 370-nm absorption band and the 420-nm emission band. Another center that should be highly dichroic is the  $M(C_{2v})$ . It should appear when  $E \parallel C$ , but we have not observed any large bands that could be attributed to this center. Perhaps because of the location of the Mg ion at the center of the unit cell, this configuration is not stable.

We have previously shown that the 400-nm absorption band is due to some type of  $M$  center. The  $M(C_1)$  center is expected to be essentially isotropic in its absorption because there are 16 different orientations permitted. Both the 400-nm absorption band and the 600 luminescence band are apparently isotropic. Therefore, we suggest that the 400-nm absorption band and the 600-nm emission band are associated with the  $M(C_1)$  center.

We feel that it is informative to interpret the temperature dependence of the peak positions and half-

widths of the bands in terms of a configuration coordinate model even though such an analysis is certainly an oversimplification. The assumptions made in this analysis are that the interaction of the defect center with the lattice can be approximated by the interaction of the defect center with a single effective vibrational mode that is a composite of all modes, that this effective mode is the same for both absorption and emission, and that the moments of the bands can be approximated by peak positions and half-widths. We have used the expression  $W_{1/2}^2(T) = W_{1/2}^2(0) \coth(h\nu/2kT)$  to find the ground  $\nu_0$  and excited  $\nu_e$  state frequencies for the  $F$  center and the  $M(C_{2h})$  center in the Sec. III.

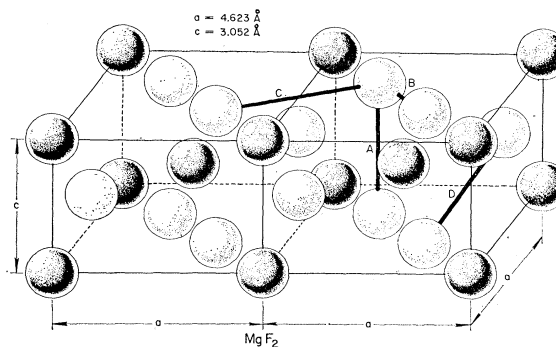


FIG. 11. The  $MgF_2$  crystal lattice.

TABLE II. Optical properties of the  $F$  and  $M(C_{2h})$  centers in  $MgF_2$ .

Defect center	Effective ground-state frequency $\nu_g$ (sec $^{-1}$ )	Effective excited-state frequency $\nu_e$ (sec $^{-1}$ )	Absorption peak (5°K) $E_p$ (eV)	Half-width 5°K $W_{1/2}$ (eV)	Huang-Rhys factor $S$
$F$	$9.0 \times 10^{12}$	...	4.929	0.597	46
$M(C_{2h})$	$8.5 \times 10^{12}$	$5.4 \times 10^{12}$	3.345	0.186	5

These frequencies along with the Huang-Rhys factors  $S$  the peak positions,  $E_p$ , and half-widths at 5°K are shown in Table II. A zero-phonon line occurs when a defect absorbs a photon without exciting any of the vibrational modes of the crystal, and the Huang-Rhys factor determines the transition probability of a zero-phonon line relative to the whole broad band associated with the defect ( $P_\infty = e^{-S}$ ). Thus, it is easily seen that as  $S$  increases the probability of observing a zero-phonon line decreases. Under the above assumptions  $S$  can be calculated from the equation  $S = [W_{1/2}(0)/2.36h\nu_g]^2$  and the Stokes shift is given by  $2Sh\nu_g$  so that  $E_{em} = E_p - 2Sh\nu_g$ . From this we find that for the  $F$  center a luminescence band at 390 nm (3.18 eV) is predicted which is directly underneath the  $M(C_{2h})$  and  $M(C_1)$  absorption. This is very close to the observed  $F$ -center luminescence at 430 nm as shown in Fig. 3. This band is so close to the 420-nm emission that one might think it is due to  $M$  centers. However,  $M$ -center luminescence is strongly polarized whereas this luminescence is not. Therefore, we attribute this emission to  $F$  centers and believe that in samples containing  $M$  centers with absorption bands at 370- and 400-nm

excitation with 254-nm light produces a broad  $F$ -center emission at about 430 nm which in turn is absorbed by the  $M$  centers and stimulates both the 420- and 600-nm luminescence. The luminescence from the center responsible for the 370-nm absorption band is, on the basis of the model, predicted to occur at 413 nm (3.0 eV). The emission is observed at 420 nm, which increases our confidence that the assignment of the 370-nm absorption and 420-nm luminescence to the same center is correct. Also, the Huang-Rhys factor of 5 for this center indicates that the zero-phonon line should be visible as indeed it is. An analysis of the temperature dependence of the 420-nm luminescence band suggests that the ground-state frequency and the excited-state frequencies differ by a factor of 1.6.

The phonon-assisted lines observed with the 370-nm absorption are due to a coupling of the defect to vibrational modes of the crystal. These modes in a crystal containing defects are of three types: Lattice modes, resonant modes, and local modes. In the case of the latter two types of modes the amplitude of the modes is a maximum at the defect, whereas the lattice modes are similar to those of a perfect crystal. In Table III an attempt has been made to assign the vibrational energies associated with phonon-assisted lines to one of these three types of modes by comparing the data with the dispersion relations calculated by Katiyar and Krishnan<sup>7</sup> for  $MgF_2$  and the measurements of Porto *et al.*<sup>8</sup> and Kahn *et al.*<sup>9</sup>

In summary we would like to reiterate the following assignments: (1) The  $F$  center absorbs light at 260 nm and emits at 430 nm. (2) The  $M(C_{2h})$  center absorbs at 370 nm and emits at 420 nm. (3) The  $M(C_1)$  center absorbs at 400 nm and emits at 600 nm.

TABLE III. Phonon-assisted transitions and zero-phonon lines in  $MgF_2$ .

Absorption peak position		Energy difference	Possible lattice mode energy assignments (cm $^{-1}$ )			Defect symmetry
nm	cm $^{-1}$		$\Gamma$	$X$	$Z$	
387.3	25820					⊥C
385.7	25927	107	92 $\Gamma_6$ ( $B_{1g}$ )	119 $X_2$		
384.5	26007	187	180 $\Gamma_6$ ( $B_{1u}$ )	209 $X_1$	186 $Z_2$	
382.7	26130	310	295 $\Gamma_9$ ( $E_g$ )	297 $X_3$		
			298 $\Gamma_{10}$ ( $E_u$ )			
			325 $\Gamma_3$ ( $A_{2g}$ )			
380.8	26261	441	438 $\Gamma_4$ ( $A_{2u}$ )	441 $X_2$	446 $Z_2$	
			450 $\Gamma_6$ ( $B_{1u}$ )	451 $X_1$		
431.6	23170					C
428.8	23321	151	Local mode?	135 $X_1$		
422.3	23680					

<sup>7</sup> R. S. Katiyar and R. S. Krishnan, Can. J. Phys. **45**, 3079 (1967).

<sup>8</sup> S. P. S. Porto, R. A. Fleury, and T. C. Damen, Phys. Rev. **154**, 522 (1967).

<sup>9</sup> R. Kahn, J. P. Trotin, D. Cribier, and C. Benoit, in Colloquium on the Inelastic Scattering of Neutrons, Copenhagen, Denmark, 1968 (unpublished).